Chin. Phys. Lett. **39**, 076101 (2022) **Express Letter**

Partially Diffusive Helium-Silica Compound under High Pressure

Cong Liu(刘聪)[1,2], Junjie Wang(王俊杰)[1], Xin Deng(邓忻)[3], Xiaomeng Wang(王晓梦)[1], Chris J. Pickard[4,5], Ravit Helled[6], Zhongqing Wu(吴忠庆)[3], Hui-Tian Wang(王慧田)[1], Dingyu Xing(邢定钰)[1], and Jian Sun(孙建)[1*]

[1]*National Laboratory of Solid State Microstructures, School of Physics and Collaborative Innovation Center of Advanced Microstructures, Nanjing University, Nanjing 210093, China*
[2]*Departament de Física, Universitat Politècnica de Catalunya, Campus Nord B4-B5, E-08034 Barcelona, Spain*
[3]*Laboratory of Seismology and Physics of Earth's Interior, School of Earth and Space Sciences, University of Science and Technology of China, Hefei 230026, China*
[4]*Department of Materials Science & Metallurgy, University of Cambridge, Cambridge CB3 0FS, UK*
[5]*Advanced Institute for Materials Research, Tohoku University, Sendai 980-8577, Japan*
[6]*Institute for Computational Science, Center for Theoretical Astrophysics & Cosmology, University of Zurich, Switzerland*

(Received 28 April 2022; accepted manuscript online 7 June 2022)

Helium is the second most abundant element in the universe, and together with silica, they are important components of giant planets. Exploring the reactivity and state of helium and silica under high pressure is crucial for understanding of the evolution and internal structure of giant planets. Here, using first-principles calculations and crystal structure predictions, we identify four stable phases of a helium-silica compound with seven/eight-coordinated silicon atoms at pressure of 600–4000 GPa, corresponding to the interior condition of the outer planets in the solar system. The density of $HeSiO_2$ agrees with current structure models of the planets. This helium-silica compound exhibits a superionic-like helium diffusive state under the high-pressure and high-temperature conditions along the isentropes of Saturn, a metallic fluid state in Jupiter, and a solid state in the deep interiors of Uranus and Neptune. These results show that helium may affect the erosion of the rocky core in giant planets and may help to form a diluted core region, which not only highlight the reactivity of helium under high pressure but also provide evidence helpful for building more sophisticated interior models of giant planets.

DOI: 10.1088/0256-307X/39/7/076101

Understanding the interiors of the giant planets in our Solar System is a key objective of planetary science and a multidisciplinary challenge combining condensed matter physics, astrophysics, and geophysics. This challenging task demands abundant accurate measurements, accompanied by theoretical models that are used to infer the planetary conditions and fit the available observational constraints. Traditional models[1–3] describe the outer planets (Jupiter, Saturn, Uranus, and Neptune) with three distinct layers: a gas-rich envelope mainly composed by hydrogen and helium, a denser convective and electrically conductive envelope that yields huge planetary magnetic fields (this layer is mainly composed of metallic fluid hydrogen for Jupiter and Saturn, and of superionic water/ammonia/methane mixture for Uranus and Neptune), together with a compact heavy element central core, with a density discontinuity at the core envelope boundary.

Thanks to updated gravity data from the Juno and Cassini missions and advance in planetary models, more complex models have been developed, in which the planetary interior is inhomogeneous and the core is diluted.[4–8] For both Jupiter and Saturn, the heavy elements could be gradually distributed or homogeneously mixed with lighter elements (hydrogen and helium) and extended to about half of the planet's total radius.[6,8] Such extended cores are difficult to explain within standard giant planet formation models,[9] and therefore it was suggested that Jupiter's fuzzy core could be a result of an energetic giant impact between a large planetary embryo with ten times Earth mass and the proto-Jupiter.[10]

However, while it is still challenging to construct accurate and unique planetary structure models for the outer giant planets, we can investigate the relevant physical and chemical processes of simple elements at high pressures and high temperatures to guide planetary interiors.[5–7,11–13] Although helium is the most inert element at ambient pressure, it can form stable compounds with other matter under high pressure. For instance, Dong *et al.*[14] have experimentally synthesized a novel Na_2He compound at around 113 GPa and 1500 K. In the deep interior of giant plan-

*Corresponding author. Email: jiansun@nju.edu.cn
© 2022 Chinese Physical Society and IOP Publishing Ltd

ets, the pressures and temperatures may provide sufficient energy for helium to form new compounds[15–19] together with other ingredients of planet interiors. Among the outer giant planets in our Solar System, another major component of the heavy elements is silica, which undergoes a series of phase transitions with compression[20–22] and may have a significant influence on the formation and evolution of terrestrial planets.[23] For the outer planets, the possible mixing or even chemical reaction of helium and silica could be important.

As aforementioned, helium and silica are major components of giant planets, nevertheless whether they can form new stable compounds under pressure and what states they can exist at giant planetary conditions are still open questions. To address these questions, we have systematically studied the helium silica system within the pressure range of planetary core conditions and found four new stable $HeSiO_2$ phases by crystal structure prediction methods and first-principles calculations. Further molecular dynamics simulations show that the $HeSiO_2$ compounds may survive inside Saturn with superionic-like helium diffusive phase and in Uranus and Neptune with solid phase, which provides more explication of the formation of diluted core in gaseous planets.

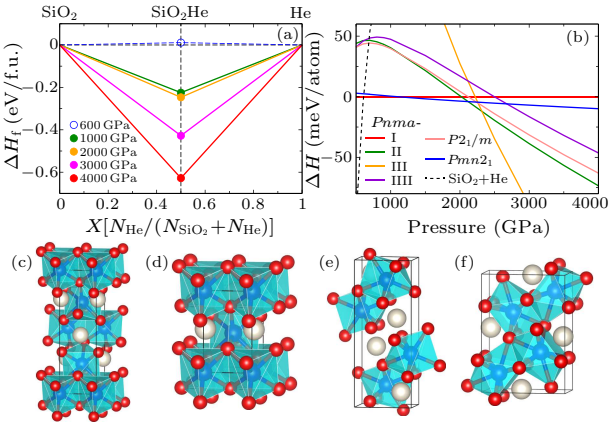

Fig. 1. Energetics of the He-SiO_2 system and crystal structures of the most stable compounds. (a) Convex hulls for formation enthalpies (ΔH_f, relative to the most stable phases of He and SiO_2[20–22]) at different pressures. (b) Enthalpies of the $HeSiO_2$ compounds of interest, as well as He-silica mixture, relative to the *Pnma*-I phase in the pressure range between 500 and 4000 GPa. (c)–(f) Crystal structure of the predicted stable $HeSiO_2$ compounds: (c) *Pnma*-I, (d) $Pmn2_1$, (e) *Pnma*-Ⅱ and (f) *Pnma*-Ⅲ, where blue, red, and silver spheres represent Si, O and He atoms, respectively.

Results. We explore the crystal structures in the helium-silica system in the pressure range of 500–4000 GPa using variable composition structure prediction method. A structure is regarded to be thermodynamically stable if its enthalpy of formation is negative relative to the mixture of the most stable phases of solid helium and silica at the corresponding pressures. As the convex hulls shown in Fig. 1(a), we find that helium and silica will form a new stable $HeSiO_2$ compound just above 600 GPa and such $HeSiO_2$ compound inclines to gain its energetic stability with further compression. We have checked the stability of the newly predicted $HeSiO_2$ compound against different exchange correlation functionals including different van der Waals (vdW) corrections, a full-potential linearized augmented plane wave (FP-LAPW) method, and zero point energy corrections, as shown in Fig. S1 of the Supplemental Material. The results demonstrate that the $HeSiO_2$ compound can survive under deep planetary pressure.

As shown in Fig. 1(b), we find several energetically competitive candidates for the $HeSiO_2$ compound. A *Pnma* phase (denoted as *Pnma*-I), will gain its stability at around 605 GPa, and then, it can transform into a $Pmn2_1$ phase at $\sim$ 1100 GPa. We find that the enthalpy of the *Pnma*-I and $Pmn2_1$ phases are pretty close, because they share the same point group and have similar crystal structures, as shown in Figs. 1(c) and 1(d). With increasing pressure, the $Pmn2_1$ phase transforms into another *Pnma* phase (denoted as *Pnma*-Ⅱ), at around 2100 GPa. Finally, a *Pnma*-Ⅲ phase, would gain its stability above 2300 GPa. Phonon calculations indicate that the above structures are all dynamically stable and temperature affects Gibbs free energy significantly for *Pnma*-Ⅱ phase, as shown in Figs. S2 and S3 of the Supplemental Material. We also calculate the electronic band gaps of these $HeSiO_2$ compounds and they are completely insulating with wide band gaps between that of He and SiO_2 crystal, as shown in Figs. S4 and S5 of the Supplemental Material. It is clear that the electronic band gaps decrease in He and SiO_2 crystals with increasing pressure. The SiO_2 crystal is predicted to transform into a semiconductor at 4 TPa and could metallize at higher pressure. Noticeably, the $HeSiO_2$ compounds have an abnormal pressure dependence with an increase in the band gap over the pressure range 500–2000 GPa. Further Bader charge (Table 1 of the Supplemental Material) calculations show that helium atoms obtain some charge (around 0.1 e) from the SiO_2 framework, which indicates that the ionic interaction may play a role in the stability of SiO_2He compounds. Previous work[22] showed that six-fold silica would transform into a mixed coordination silica with an averaged coordination number of 8 by compression. Interestingly, in our newly found $HeSiO_2$ compound, all silicon atoms in *Pnma*-I, $Pmn2_1$, and *Pnma*-Ⅱ phases are seven-fold coordinated with oxygen atoms, while *Pnma*-Ⅲ phase is purely eight-fold. These seven-fold and eight-fold configurations are rare in pure silica, which indicates that the inserting of helium atoms can significantly change the packing of sil-

icon and oxygen atoms, as well as the silicon-oxygen bonding behaviors. Meanwhile, we also find that a purely eight-fold $HeSiO_4$ compound with $I\bar{4}22$ phase can survive above 400 GPa, as shown in Figs. S6 and S7 of the Supplemental Material. This may shed light on further explorations on chemical coordination in helium compounds.

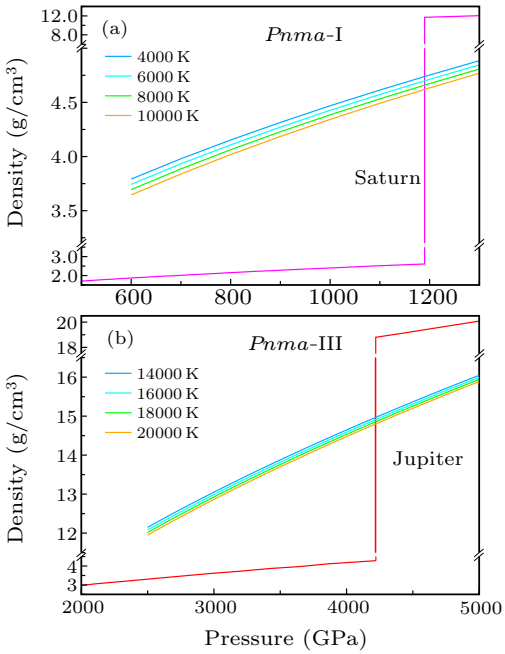

Fig. 2. Compression curves of the $HeSiO_2$ compound: (a) *Pnma*-I phase, (b) *Pnma*-Ⅲ phase. Colorful continuous lines represent *ab initio* results at variable temperatures, while the discontinuous lines represent density-pressure curves of different planetary interiors: Jupiter[24] (red), Saturn[25] (magenta).

Since $HeSiO_2$ compound could exist in high pressure range corresponding to deep interiors of giant planets, we investigated the equation of state of the $HeSiO_2$ compound, as shown in Fig. 2. In the traditional 3-layer models for of Jupiter and Saturn with distinct layers, their density curves increase sharply at core mantle boundary. Our *ab initio* calculations show that the density curves of the $HeSiO_2$ compound have a smooth tendency: increasing by compression, while decreasing by heating. Most importantly, they are located just between that of the core and mantle, which indicates that the newly found $HeSiO_2$ compound very possibly exists near the core mantle boundary of giant gaseous planets, such as Jupiter and Saturn. Especially when consider diluted core models, helium/hydrogen is expected to erode the core and their density curves would change to a smooth one, which should agree with the density of states of the $HeSiO_2$ compound even more closely, in the deep interiors of Jupiter and Saturn.

In order to gain a better understanding of such $HeSiO_2$ compound affecting the interior model of giant planets, one should account for both the equation of states calculations and the pressure-temperature phase diagrams, because the internal structure models must be consistent with the phase diagram of the assumed materials and their dynamical behavior. We perform extensive *ab initio* molecular dynamics (AIMD) simulations at deep planetary conditions to study the dynamical properties of our predicted $HeSiO_2$ compound. Diffusion coefficients (D) were calculated for the silicon, oxygen, and helium atoms from the averaged mean-square displacements (MSD) to monitor different types of atomic motions ($D = \partial\mathrm{MSD}/\partial t$). We demonstrated the atomic trajectories from simulations at the initial pressure of 600 GPa for the *Pnma*-I phase $HeSiO_2$ compound as an example, as shown in Fig. S8 of the Supplemental Material. At 5000 K, all atoms oscillate around their equilibrium positions, resulting in three horizontal MSD curves with slightly oscillating ($D = 0$). When heating up to 9000 K, we find that the helium atoms became diffusive freely within the static silica frameworks during the simulations ($D_{\mathrm{He}} > D_{\mathrm{O}} = D_{\mathrm{Si}} = 0$). These are clearly two different states: the solid phase at 5000 K and the superionic-like partial diffusive phase at 9000 K.

Inspired by this helium diffusive state in the $HeSiO_2$ compound, we extended the pressure and temperature range of our AIMD simulations to explore the states of the $HeSiO_2$ compound under the deep interior condition of Saturn and Jupiter, as shown in Fig. 3. Each colored symbol corresponds to an independent simulation to avoid correlation effects, and the pressures and temperatures were obtained from simulations by statistically averaging. Due to the different stable pressure range of $HeSiO_2$ phases, as well as the core mantle boundary conditions of Saturn (1 TPa and 10000 K) and Jupiter (4 TPa and 20000 K) varying a lot, we separately simulate $HeSiO_2$ compounds in pressure range of 500–1200 GPa with *Pnma*-I phase [as shown in Fig. 3(a)] and in pressure range of 2000–5000 GPa with *Pnma*-Ⅲ phase [as shown in Fig. 3(b)] up to the melting temperature. It is clear that the superionic-like helium diffusive state is widespread at high pressure and high temperature and exists between the solid phase and fluid phase in the $HeSiO_2$ phase diagram. With increasing pressure, this helium diffusive state appears at higher temperatures.

For comparison, the isentropes of the giant outer planets (Jupiter, Saturn, Uranus, and Neptune) are also plotted in Fig. 3 to represent the pressure temperature profiles at deep interior conditions. We find that the pressure temperature profile of Saturn (magenta) perfectly passes through the superionic-like helium diffusive region of the $HeSiO_2$ compound, which suggests that such helium diffusive $HeSiO_2$ compound can exist near the core mantle boundary of Saturn. As for Jupiter, both adiabatic (red) and non-

adiabatic (white) pressure temperature profiles are slightly higher than the helium diffusive region. In other words, the $HeSiO_2$ compound is totally melted in the core region, if we account for a diluted core model of Jupiter. Previous works[26,27] on typical mantle silicates (MgO, SiO_2, and $MgSiO_3$) showed that upon melting, the behavior of SiO_2 changes from semi-conducting to semi-metallic, indicating that a magnetic dynamo process would develop in the magma oceans of Super-Earths. We calculate the electronic density of states (DOS) of $HeSiO_2$ compounds at different temperatures and find that at higher temperature $HeSiO_2$ compounds may also transform into metallic in fluid state, which may affect the conductivity and therefore the magnetic field generation in Jupiter. The pressure temperature profiles of Uranus and Neptune are much lower than that of Jupiter and Saturn, and in this case the $HeSiO_2$ compounds may exist in solid form in the deep interior of Uranus and Neptune when helium deposits and erode the core.

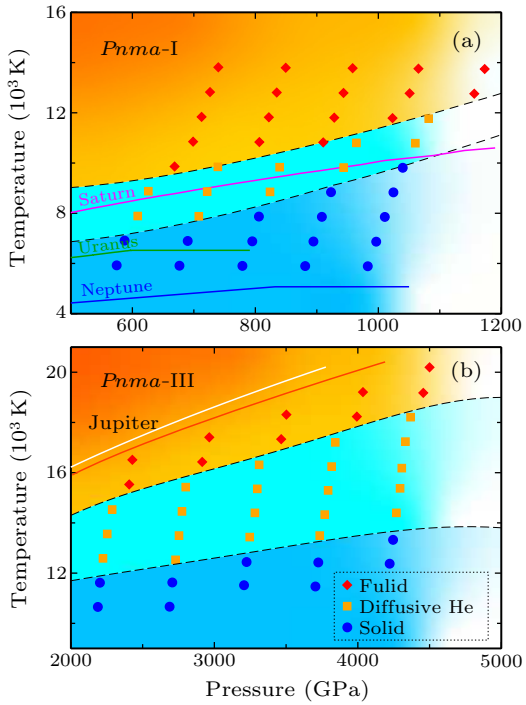

Fig. 3. Proposed phase diagram of the $HeSiO_2$ compound: (a) *Pnma*-I phase and (b) *Pnma*-Ⅲ phase under planetary interior conditions by AIMD simulations. The simulations are marked with three different symbols: blue circle, orange square, and red diamond represent the solid, helium diffusive, and fluid states, respectively. Black dashed lines are fitted to the phase transition boundaries. The pressure-temperature profiles for giant planets are plotted in red (Jupiter[24]), magenta (Saturn[25]), dark green (Uranus[28]), and blue (Neptune[28]) for reference, assuming adiabatic interiors. A profile for the non-adiabatic Jupiter model (white)[4] is also provide for comparison.

We also calculate the elastic and wave velocity properties of the $HeSiO_2$ compound to explore how it affects the evolution of the interior of Uranus and Neptune. The calculated bulk moduli (K_S), shear moduli (G), compressional velocities (V_P), and shear wave velocities (V_S) of the *Pnma* phase $HeSiO_2$ compound, as well as pure helium and silica for comparison, at pressures 500–1000 GPa are shown in Fig. 4. He and $HeSiO_2$ compound both have almost linear temperature and pressure dependences of bulk moduli and shear moduli. For instance, in the $HeSiO_2$ compound, the first temperature and pressure derivate of elastic properties almost keep unchanged ($\partial K_S/\partial T = -0.013$ GPa/K, $\partial G/\partial T = -0.016$ GPa/K, $\partial K_S/\partial P = 2.7$, and $\partial G/\partial P = 1.1$). In contrast, noticeable nonlinear dependences on temperature and pressure are observed for the wave velocities. Comparing with pure silica, the penetration of helium into silica can reduce the compressibility as the previous report in helium-silica mixture.[29]

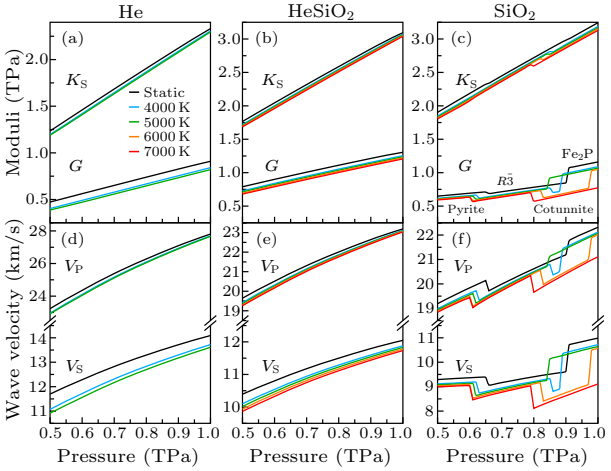

Fig. 4. Comparisons of elastic moduli and wave velocities between pure He, the *Pnma* phase $HeSiO_2$ compound, and SiO_2 along the pressure-temperature profiles for Uranus and Neptune. Elastic moduli and wave velocities. (a)–(c) Bulk and shear moduli (K_S and G), (d)–(f) compressional and shear wave velocities (V_P and V_S). Colorful lines represent the *ab initio* results at various temperatures.

The chemical composition can also affect the elastic moduli and wave velocities of these planetary matters. Although pure helium has a pretty small bulk moduli and shear moduli, helium has larger compressional velocities and shear wave velocities than silica and $HeSiO_2$ due to its small density ($V_P = \sqrt{(K_S + \frac{4}{3}G)/\rho}$ and $V_S = \sqrt{G/\rho}$, where ρ is density). In silica, the Cotunnite-type phase surviving in high temperature region has a small shear moduli and shear wave velocities with respect to other phases, which indicates that an ultralow-velocity zones may exist in the mantle of super-earth. Compared to silica, $HeSiO_2$ has a slightly smaller bulk moduli but larger shear moduli. Due to the decrease of density by inserting helium, the velocities of $HeSiO_2$ compound have a larger compressional velocities and shear wave velocities than that of silica. Notably, the temperature does not significantly affect wave velocities. For instance,

wave velocities vary 0.16 and 0.23 km/s for compressional velocities and shear wave velocities from 4000 K to 7000 K at 500 GPa and these differences are evidently diminished at high pressure, which decrease to 0.08 and 0.14 km/s at 1000 GPa. Thus, the inserting of helium may evidently increase the wave velocities of silica and our newly predicted $HeSiO_2$ may affect the model of the deep interior of Uranus and Neptune.

Discussion. The composition of giant planets cannot be measured directly. Instead, their bulk compositions and internal structures can only be inferred indirectly from interior models that fit the available measured physical parameters. Here we used the calculated equations of state (EoS) of our predicted $HeSiO_2$ compound to derive the density (as shown in Fig. 2.) and the associated pressure temperature phase diagram (as shown in Fig. 3), and then we attempt to sketch internal structure models for Jupiter, Saturn, Uranus, and Neptune.

Our static calculations show that helium and silica can react with each other in the deep interiors of giant planets, and the $HeSiO_2$ compounds may survive near the core mantle boundary of giant planets. Especially considering that helium may be immiscible with hydrogen at 1–2 MBar, namely "helium rain", it is expected to settle down into deep interior of Jupiter and Saturn. Thus, helium in the deep interior could affect the erosion of the compact heavy-element core, which may result in a gradually expanding core region and forming a diluted one. Here, we only fitted density curves and pressure temperature phase diagram of the $HeSiO_2$ compound to the representative planetary models, more physical data (such as their masses, radii, gravitational and magnetic fields, 1-bar temperatures, atmospheric composition, and internal rotations) of planets are required to construct a more comprehensive model. Moreover, it should be noted that other elements may influence the stability of silica at high pressure as well, for instance, the hydrogen can also react with silica at high pressure, as we discussed elsewhere.[12] However, a complete investigation in the H–He–Si–O system or more complicated systems with other elements is beyond the scope of this work.

In summary, using crystal structure prediction and *ab initio* calculations, we have predicted four phases of $HeSiO_2$ compound (*Pnma*-I, $Pmn2_1$, *Pnma*-II, and *Pnma*-III), which can gain their stability in the pressure range of 600–4000 GPa, corresponding to deep interior conditions of giant planets, such as Jupiter, Saturn, Uranus, and Neptune. Due to the spatial occupation of helium atoms, the silicon atoms in these compounds are all bonded to seven/eight oxygen atoms, which are very rare cases in pure silica. Thus, helium and other inert gas atoms can be used as a space filler to design compounds with usual chemical bonding and coordination under high pressure. Equation of states calculations suggests that the density curves of our newly predicated $HeSiO_2$ compound are close to current models of Jupiter and Saturn, especially when accounting for diluted core models. Furthermore, extensive *ab initio* molecular dynamics simulations illustrated that the $HeSiO_2$ compound can survive in the helium diffusive state under the core-mantle boundary conditions of Saturn and metallic fluid state under the core-mantle boundary conditions of Jupiter, which may shed light on the formation or evolution of diluted core of such gaseous giants. Noticeably, under the pressure-temperature conditions in the deep interiors of Uranus and Neptune, the $HeSiO_2$ compound is found to be in solid form due to lower temperatures. We also carried out elastic and wave velocity properties calculations for the $HeSiO_2$ compound in the pressure range 500–1000 GPa and found that the inserting of helium increases the compressional and shear wave velocities in the core region of Uranus and Neptune. Our findings may be used to guide future shock wave compression experiments and giant planet interior models, as well as to significantly improve our understanding on giant planets in the solar system and exoplanets.

Methods. We used Magus (machine learning and graph theory assisted universal structure searcher) code to search for the crystal structures, in which we employed the Bayesian optimization[30] and graph theory[31] to improve the search efficiency and diversity. We performed extensive crystal structure searches on $He_x(SiO_2)_y$ (x = 1–4, y = 1–4) at 500, 1000, 2000, and 4000 GPa with maximum atom number up to 40. Meanwhile we also performed ternary variable composition crystal structure searches on $He_xSi_yO_z$. Some compositions are further double checked with extensive fixed composition searches. Each search runs over 25 generations and each generation has a population size of 60 structures. There are 40%–60% of the parents for the evolution of next generation from the lowest enthalpy structures of the last generation, and the left seeds are randomly produced. We also cross checked the searching results with AIRSS[32,33] combined with CASTEP.[34]

DFT calculations were performed with the Vienna *ab initio* simulation package (VASP),[35] accompanied with the projector augmented-wave (PAW) method.[36] We chose $3s^23p^2$, $2s^22p^4$, and $1s^2$ as valence electrons for Si, O, and He, and used the generalized gradient approximation (GGA) in the Perdew–Burke–Ernzerhof exchange correlation functional.[37] All predicted structures were further optimized by the hard version pseudopotentials and employed a plane wave cutoff of 1050 eV and dense Monkhorst–Pack k-point sampling grids with resolutions of $2\pi \times 0.025$ Å^{-1}, leading to ionic and cell optimizations with energy and force convergences better than 10^{-6} eV

and 0.002 eV/Å, respectively. The CASTEP code[34] was used for the *ab initio* random structure searching approach searches. Similar convergence parameters as used in the Vienna *ab initio* simulation package were employed.

Elastic properties at high pressure and temperature are calculated by *cij* package[38] based on phonon spectrum from the PHONONPY package.[39] The static elastic constants are calculated by the stress strain method. We should notice that the calculated results of elastic properties will be influenced by temperature, and calculations based on the quasi-harmonic approximation will be invalid in the superionic/fluid state where some atoms can diffuse freely.

We adopted the canonical NVT ensemble using a Nose–Hoover thermostat[40] to perform *ab initio* molecular dynamics (AIMD) simulations in a supercell with 192 atoms for both *Pnma*-I phase and *Pnma*-Ⅲ phase, with Γ-centered k-points sampling, normal version pseudopotentials and a cutoff energy of 720 eV were adopted to ensure energy convergence of better than 10^{-5} eV. Each simulation lasts for 12 ps with a time step of 1 fs, and we allowed the first 2 ps for thermalization. We tested the influence from box size and k-mesh choice, as shown in Table 2 of the Supplemental Material. DOS at definite temperatures is estimated by averaging over 10 configurations from molecular dynamics trajectory.

Acknowledgements. J.S. gratefully acknowledges the financial support from the National Natural Science Foundation of China (Grant Nos. 12125404, 11974162, and 11834006), and the Fundamental Research Funds for the Central Universities. The calculations were carried out using supercomputers at the High Performance Computing Center of Collaborative Innovation Center of Advanced Microstructures, the high-performance supercomputing center of Nanjing University.

References

[1] Saumon D and Guillot T 2004 *Astrophys. J.* **609** 1170
[2] Redmer R, Mattsson T R, Nettelmann N and French M 2011 *Icarus* **211** 798
[3] Bethkenhagen M, Meyer E R, Hamel S, Nettelmann N, French M, Scheibe L, Ticknor C, Collins L A, Kress J D, Fortney J J and Redmer R 2017 *Astrophys. J.* **848** 67
[4] Debras F and Chabrier G 2019 *Astrophys. J.* **872** 100
[5] Helled R, Nettelmann N and Guillot T 2020 *Space Sci. Rev.* **216** 38
[6] Helled R 2019 *The Interiors of Jupiter and Saturn* in *Oxford Research Encyclopedias: Planetary Science* (Oxford: Oxford University Press)
[7] Vazan A, Sari R and Kessel R 2020 arXiv:2011.00602 [astro-ph.EP]
[8] Mankovich C and Fuller J 2021 arXiv:2104.13385 [astro-ph.EP]
[9] Müller S, Helled R and Cumming A 2020 *Astron. Astrophys.* **638** A121
[10] Liu S F, Hori Y, Müller S, Zheng X, Helled R, Lin D and Isella A 2019 *Nature* **572** 355
[11] Cavazzoni C, Chiarotti G L, Scandolo S, Tosatti E, Bernasconi M and Parrinello M 1999 *Science* **283** 44
[12] Gao H, Liu C, Shi J, Pan S, Huang T, Lu X, Wang H T, Xing D and Sun J 2022 *Phys. Rev. Lett.* **128** 035702
[13] Li H F, Oganov A R, Cui H, Zhou X F, Dong X and Wang H T 2022 *Phys. Rev. Lett.* **128** 035703
[14] Dong X, Oganov A R, Goncharov A F, Stavrou E, Lobanov S, Saleh G, Qian G R, Zhu Q, Gatti C, Deringer V L, Dronskowski R, Zhou X F, Prakapenka V B, Popov Z K I A, Boldyrev A I and Wang H T 2017 *Nat. Chem.* **9** 440
[15] Liu C, Gao H, Wang Y, Needs R J, Pickard C J, Sun J, Wang H T and Xing D 2019 *Nat. Phys.* **15** 1065
[16] Bai Y H, Liu Z, Botana J, Yan D D, Lin H Q, Sun J, Pickard C J, Needs R J and Miao M S 2019 *Commun. Chem.* **2** 102
[17] Liu C, Gao H, Hermann A, Wang Y, Miao M, Pickard C J, Needs R J, Wang H T, Xing D and Sun J 2020 *Phys. Rev. X* **10** 021007
[18] Gao H, Liu C, Hermann A, Needs R J, Pickard C J, Wang H T, Xing D and Sun J 2020 *Natl. Sci. Rev.* **7** 1540
[19] Shi J, Cui W, Hao J, Xu M, Wang X and Li Y 2020 *Nat. Commun.* **11** 3164
[20] Tsuchiya T and Tsuchiya J 2011 *Proc. Natl. Acad. Sci. USA* **108** 1252
[21] Wu S, Umemoto K, Ji M, Wang C Z, Ho K M and Wentzcovitch R M 2011 *Phys. Rev. B* **83** 184102
[22] Liu C, Shi J, Gao H, Wang J, Han Y, Lu X, Wang H T, Xing D and Sun J 2021 *Phys. Rev. Lett.* **126** 035701
[23] Umemoto K, Wentzcovitch R M and Allen P B 2006 *Science* **311** 983
[24] Miguel Y, Guillot T and Fayon L 2016 *Astron. Astrophys.* **596** A114
[25] Helled R and Guillot T 2013 *Astrophys. J.* **767** 113
[26] Millot M, Dubrovinskaia N, Černok A, Blaha S, Dubrovinsky L, Braun D G, Celliers P M, Collins G W, Eggert J H and Jeanloz R 2015 *Science* **347** 418
[27] Soubiran F and Militzer B 2018 *Nat. Commun.* **9** 3883
[28] Nettelmann N, Helled R, Fortney J J and Redmer R 2013 *Planet. Space Sci.* **77** 143
[29] Sato T, Funamori N and Yagi T 2011 *Nat. Commun.* **2** 345
[30] Xia K, Gao H, Liu C, Yuan J, Sun J, Wang H T and Xing D 2018 *Sci. Bull.* **63** 817
[31] Gao H, Wang J, Guo Z and Sun J 2020 *npj Comput. Mater.* **6** 143
[32] Pickard C J and Needs R J 2006 *Phys. Rev. Lett.* **97** 045504
[33] Pickard C J and Needs R J 2011 *J. Phys.: Condens. Matter* **23** 053201
[34] Clark S J, Segall M D, Pickard C J, Hasnip P J, Probert M I J, Refson K and Payne M C 2005 *Z. Krist. -Cryst. Mater.* **220** 567
[35] Kresse G and Furthmüller J 1996 *Phys. Rev. B* **54** 11169
[36] Blöchl P E 1994 *Phys. Rev. B* **50** 17953
[37] Perdew J P, Burke K and Ernzerhof M 1996 *Phys. Rev. Lett.* **77** 3865
[38] Luo C, Deng X, Wang W, Shukla G, Wu Z and Wentzcovitch R M 2021 *Comput. Phys. Commun.* **267** 108067
[39] Togo A and Tanaka I 2015 *Scr. Mater.* **108** 1
[40] Hoover W G 1985 *Phys. Rev. A* **31** 1695

Supplementary Information for "Partially Diffusive Helium-Silica Compound under High Pressure"

Cong Liu (刘聪),[1,2] Junjie Wang (王俊杰),[1] Xin Deng (邓忻),[3] Xiaomeng Wang (王晓梦),[1] Chris J. Pickard,[4,5] Ravit Helled,[6] Zhongqing Wu (吴忠庆),[3] Hui-Tian Wang (王慧田),[1] Dingyu Xing (邢定钰),[1] and Jian Sun (孙建)[1,*]

[1] *National Laboratory of Solid State Microstructures, School of Physics and Collaborative Innovation Center of Advanced Microstructures, Nanjing University, Nanjing, 210093, China*

[2] *Departament de Física, Universitat Politècnica de Catalunya, Campus Nord B4-B5, E-08034 Barcelona, Spain*

[3] *Laboratory of Seismology and Physics of Earth's Interior, School of Earth and Space Sciences, University of Science and Technology of China, Hefei, China*

[4] *Department of Materials Science & Metallurgy, University of Cambridge, 27 Charles Babbage Road, Cambridge CB3 0FS, UK*

[5] *Advanced Institute for Materials Research, Tohoku University 2-1-1 Katahira, Aoba, Sendai, 980-8577, Japan*

[6] *Institute for Computational Science, Center for Theoretical Astrophysics & Cosmology, University of Zurich, Switzerland*

[*] Corresponding author. jiansun@nju.edu.cn

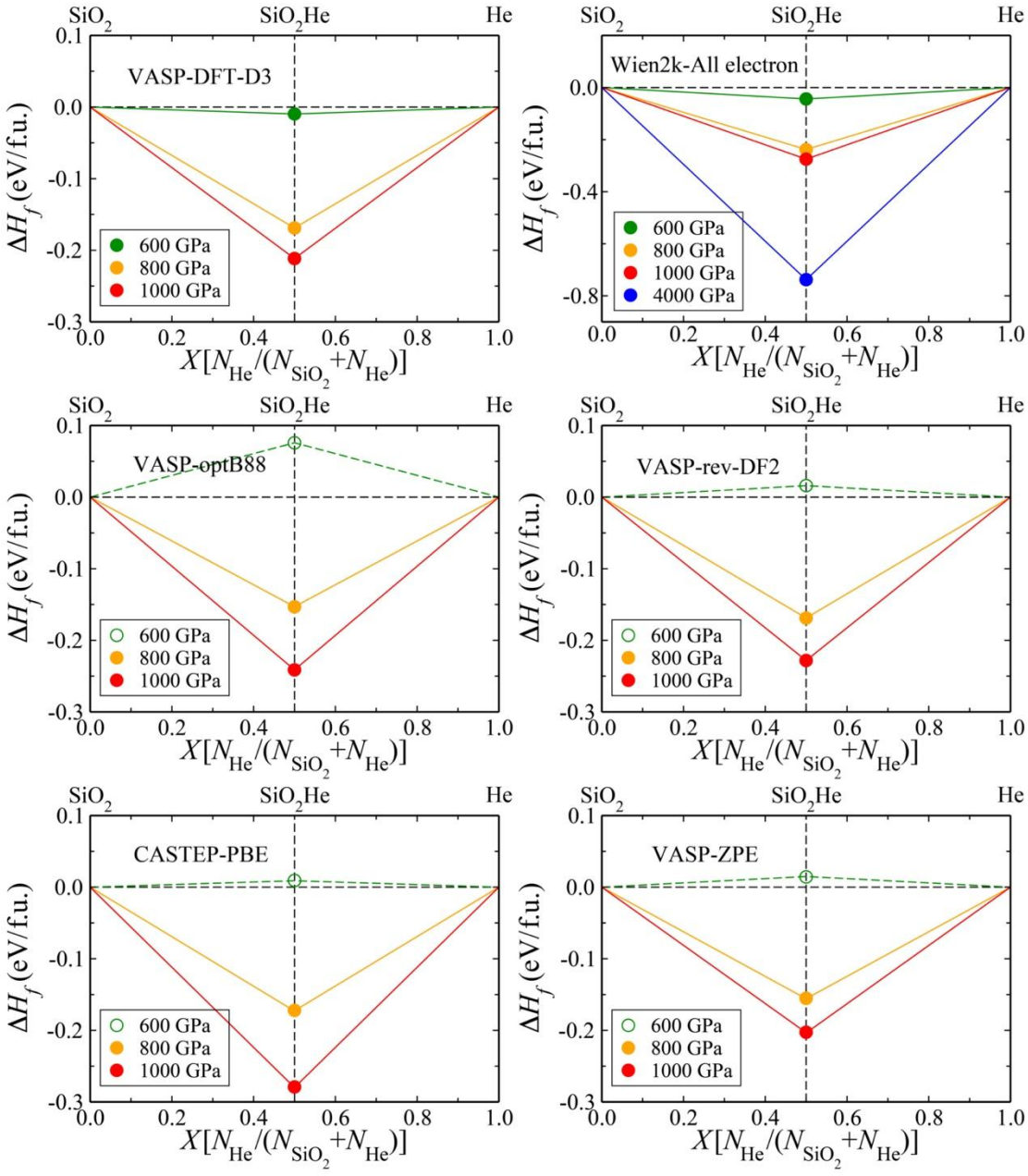

Fig. S1. Convexhull of formation enthalpies (ΔH_f) calculated from DFT-D3[1], all electron potentials (Wien2k[2]), vdw-optB88[3] and rev-vdw-DF2[4], CASTEP[5], and with zero point energy (ZPE). The results are robust and consistent with different functionals and methods.

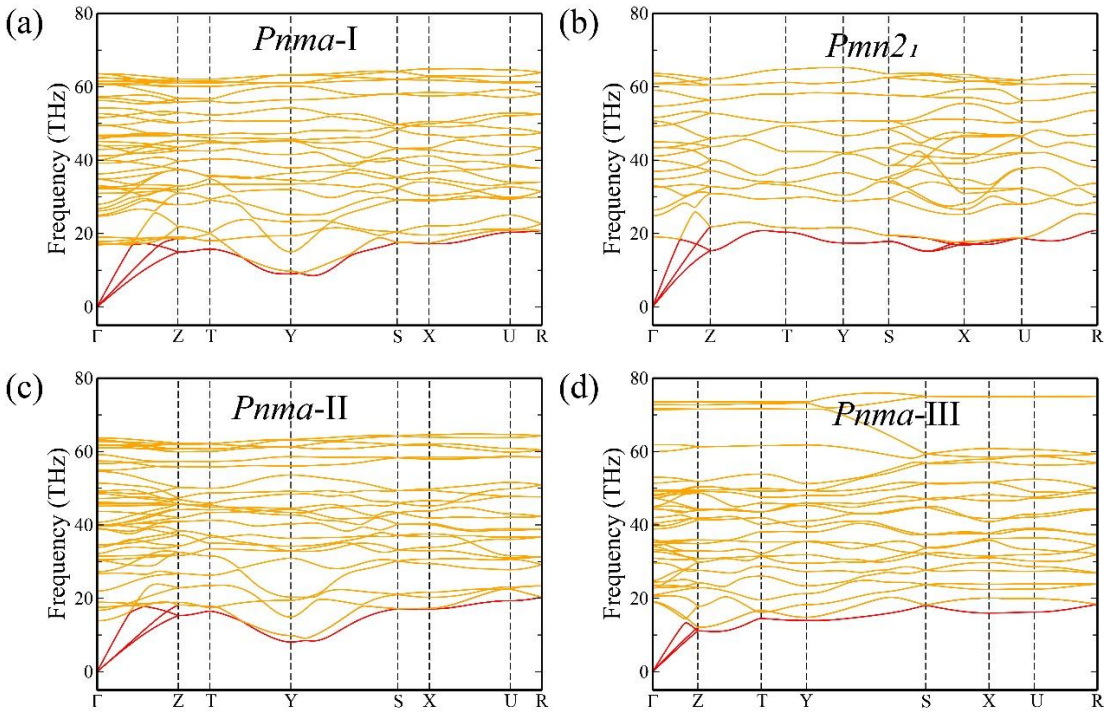

Fig. S2. Calculated Phonon spectra of the thermodynamically stable/metastable phases: (a) *Pnma*-I, (b) *Pmn2₁*, (c) *Pnma*-II, and (d) *Pnma*-III. The orange curves correspond to optical branches and the red curves correspond to acoustic branches. No imaginary vibrational frequencies were found in the phonon spectra.

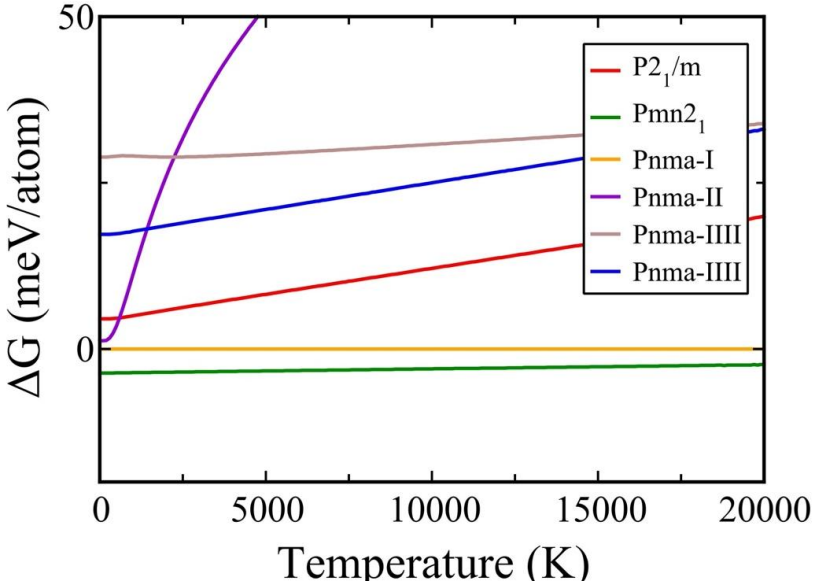

Fig. S3. Gibbs free energy at 2000 GPa based on QHA calculations.

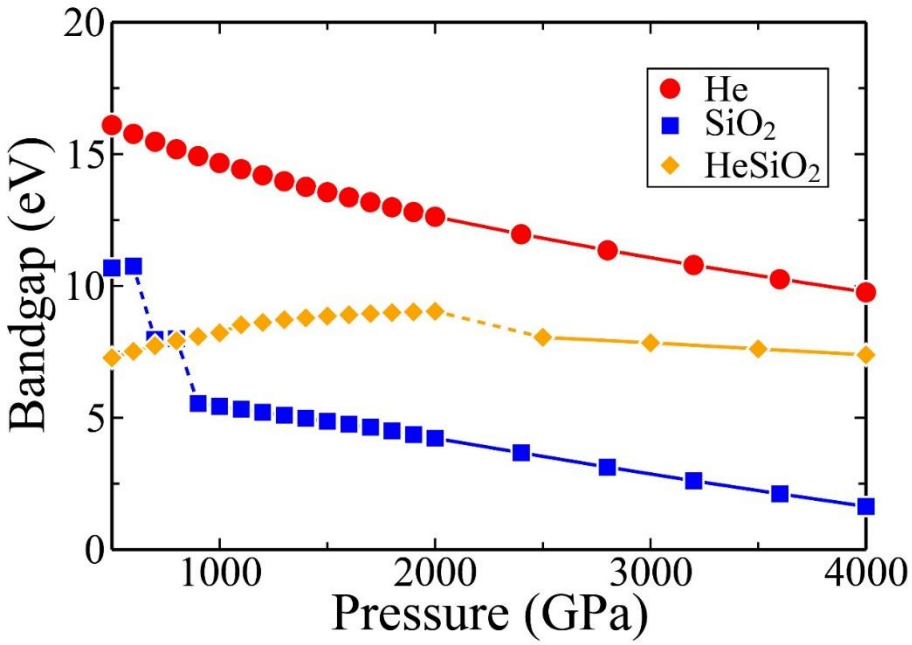

Fig. S4. Calculated Band gaps of He, SiO_2, and $HeSiO_2$ over the pressure range 500-4000 GPa based on simply pure PBE functional.

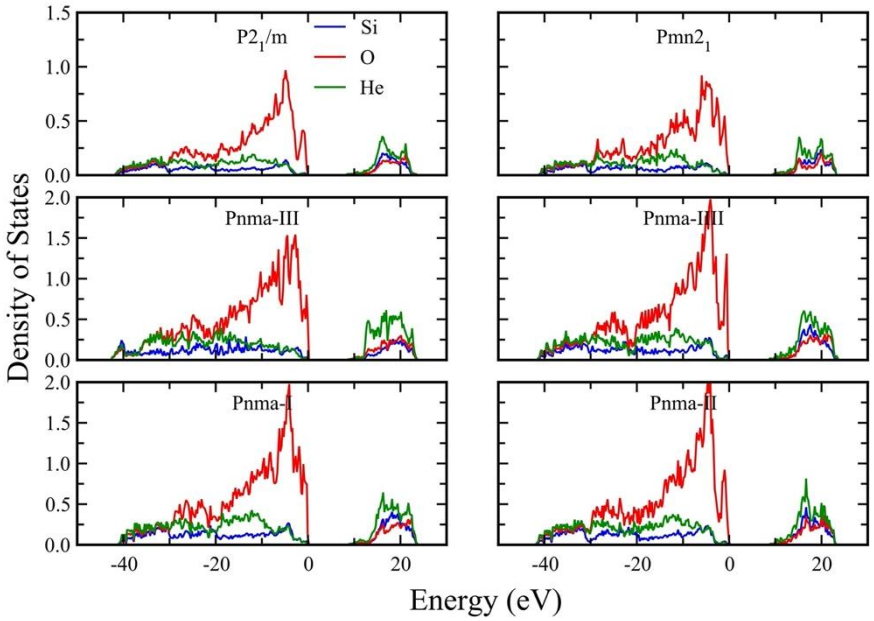

Fig. S5. Density of states for all $HeSiO_2$ canidates at 2000 GPa based on simply pure PBE functional.

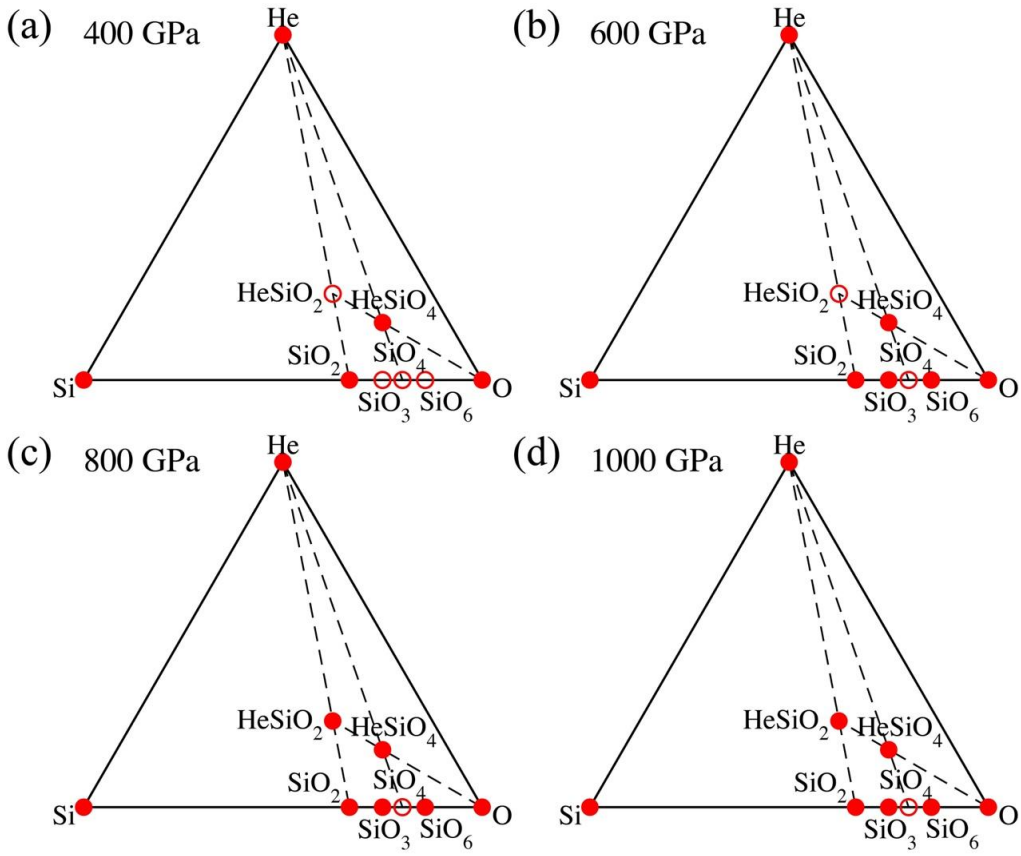

Fig. S6. Ternary phase diagram of the He-Si-O system at 400, 600, 800, and 1000 GPa. The stable/unstable phases are marked in solid/open red points.

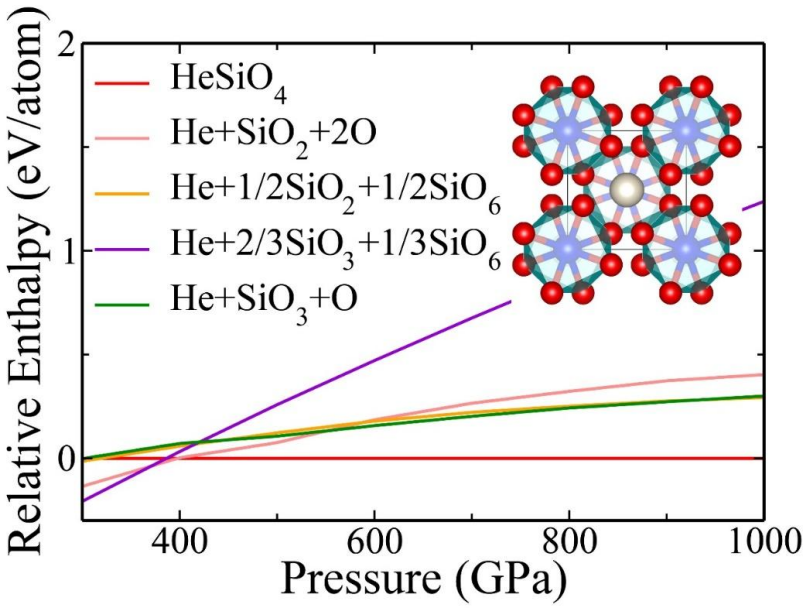

Fig. S7. Enthalpies of the $HeSiO_4$ compounds, as well as its possible decompositions in the pressure range between 300 and 1000 GPa. Insert figure show the crystal structure of *I422* phase $HeSiO_4$.

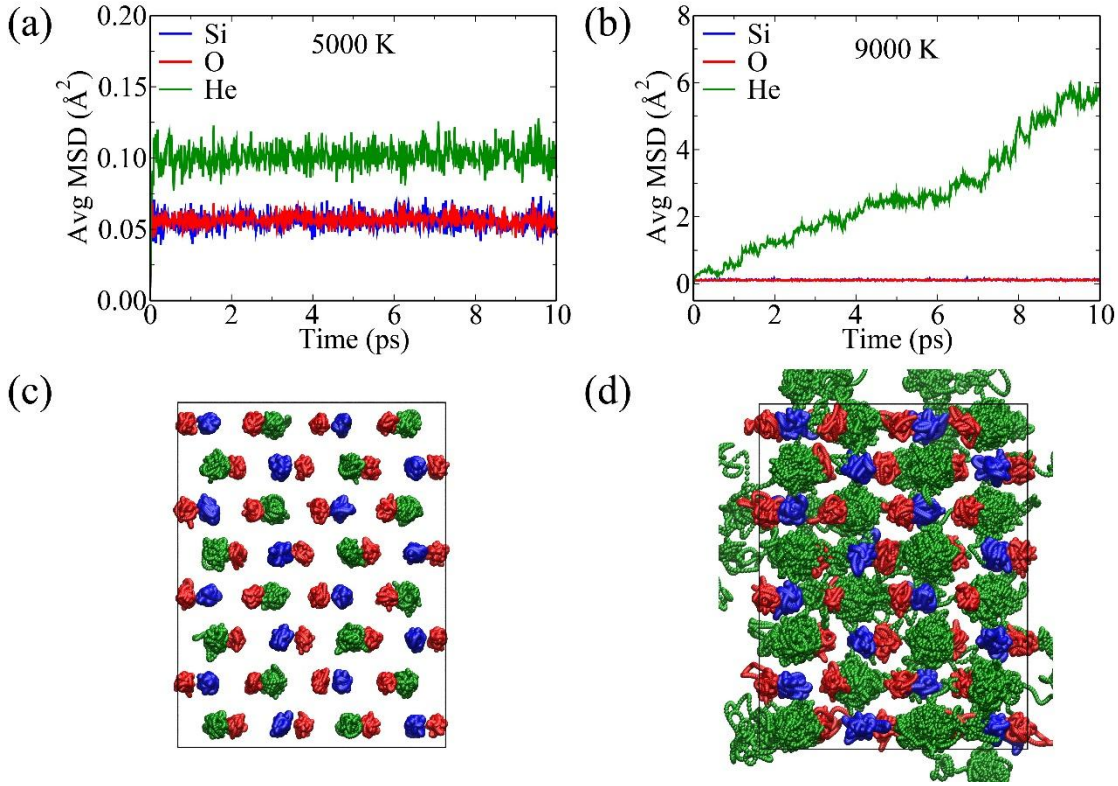

Fig S8. Dynamical behavior of Si (blue), O (red), and He atoms (dark green) in the $HeSiO_2$ compound under high pressures and high temperatures. AIMD simulations were performed at initial pressure of 600 GPa for the *Pnma* $HeSiO_2$ compound. (a-b) The averaged mean-squared displacements (MSD). (c-d) Atomic trajectories from the simulations representing the plastic phase. The Si, O and He atoms are respectively plotted with blue, red, and dark green.

Table I. Bader charge on helium atoms in different phases.

Pressure	$P2_1/m$	$Pmn2_1$	Pnma-III	Pnma-IIII	Pnma-I	Pnma-II
500 GPa	2.075	2.078	2.072	2.079	2.078	2.075
1000 GPa	2.088	2.085	2.069	2.090	2.083	2.087
2000 GPa	2.095	2.083	2.056	2.089	2.088	2.093
3000 GPa	2.105	2.079	2.064	2.106	2.082	2.083
4000 GPa	2.112	2.090	2.074	2.116	2.092	2.079

Table II. Thermodynamic data from our simulations affect by different box size (number of atoms in supercells: *N*) and *k-mesh* on motion behaviors of each species of atom in *Pnma*-I phase.

V (Å^3)	T (K)	P (GPa)	N	*k-mesh*	D_{Si} D_O D_{He} ($10^{-8}\ m^2/s$)	State
659.04	5000	663.84	192	$1 \times 1 \times 1$	0.00 0.00 0.00	Solid
659.04	5000	663.97	192	$2 \times 2 \times 2$	0.00 0.00 0.00	Solid
1318.09	5000	663.93	384	$1 \times 1 \times 1$	0.00 0.00 0.00	Solid
659.04	9000	721.66	192	$1 \times 1 \times 1$	0.00 0.00 0.12	*SI*
659.04	9000	719.64	192	$2 \times 2 \times 2$	0.00 0.00 0.10	*SI*
1318.09	9000	721.45	384	$1 \times 1 \times 1$	0.00 0.00 0.08	*SI*
659.04	9000	820.87	192	$1 \times 1 \times 1$	1.08 1.48 3.37	Fluid
659.04	12000	822.06	192	$2 \times 2 \times 2$	1.07 1.51 4.02	Fluid
1318.09	12000	820.75	384	$1 \times 1 \times 1$	1.06 1.40 3.98	Fluid

Table III. Structural information for $HeSiO_2$ compounds at 1000 GPa.

Space group	Lattice parameters (Å)	Atomic coordinates (fractional)	
Pnma-I	a = 7.3530 b = 2.2022 c = 2.8982	Si	0.6125 0.7500 0.2546
		O	0.9667 0.2500 0.2499
		O	0.2153 0.2500 0.0276
		He	0.3531 0.7500 0.0657
Pnma-II	a = 7.4130 b = 2.1865 c = 2.8849	Si	0.8618 0.7500 0.5341
		O	0.0339 0.7500 0.2387
		O	0.2835 0.7500 0.4700
		He	0.1023 0.7500 0.7868
Pnma-III	a = 3.9635 b = 2.1028 c = 5.5564	Si	0.8139 0.7500 0.1580
		O	0.6865 0.7500 0.4528
		O	0.9774 0.7500 0.7208
		He	0.4570 0.2500 0.9751
Pnma-IV	a = 5.4683 b = 2.1832 c = 3.9197	Si	0.3271 0.2500 0.1362
		O	0.3930 0.7500 0.8795
		O	0.6083 0.2500 0.6175
		He	0.6496 0.7500 0.3703
$Pmn2_1$	a = 2.2011 b = 3.6785 c = 2.8973	Si	0.0000 0.7249 0.7610
		O	0.0000 0.0697 0.4804
		O	0.5000 0.4334 0.7582
		He	0.5000 0.7940 0.4424
$P2_1/m$	a = 2.8890 b = 2.1869 c = 4.0453	Si	0.3805 0.7500 0.7236
		O	0.2124 0.2500 0.4332
		O	0.7235 0.2500 0.9325
		He	0.0984 0.2500 0.7953

Table V. Structural information for $HeSiO_4$ compounds at 1000 GPa.

Space group	Lattice parameters (Å)	Atomic coordinates (fractional)	
I422	a = 3.2944	Si	0.5000 0.5000 0.5000
		O	0.6312 0.8688 0.7500
		He	0.5000 0.5000 0.0000

Reference

1. Grimme, S., Ehrlich, S. & Goerigk, L. Effect of the damping function in dispersion corrected density functional theory. *J. Comput. Chem.* **32**, 1456–1465 (2011).
2. Blaha, P., Schwarz, K., Kvasnicka, D. & Luitz, J. WIEN2k: An Augmented Plane Wave Plus Local Orbitals Program for Calculating Crystal Properties (Karlheinz Schwarz, Technische Universitaet Wien, Vienna, 2001).
3. Klimeš, J., Bowler, D. R. & Michaelides, A. Chemical accuracy for the van der Waals density functional. *J. Phys. Condens. Matter* **22**, 022201 (2009).
4. Hamada, I. van der Waals density functional made accurate. *Phys. Rev. B* **89**, 121103 (2014).
5. Clark, S. J. *et al.* First principles methods using CASTEP. *Z. Für Krist. - Cryst. Mater.* **220**, 567–570 (2009).